[논 문] 한국재료학회지
Kor. J. Mater. Res.
Vol. 19, No. 9 (2009)

DOI: 10.3740/MRSK.2009.19.9.481

Characterization of Methylene Blue Decomposition on Fe-ACF/TiO_2 Photocatalysts Under UV Irradiation with or Without H_2O_2

Kan Zhang and Won-Chun Oh*

Department of Advanced Materials & Science Engineering, Hanseo University, Chungnam 356-706, Korea

(Received June 22, 2009 : Received in revised form August 20, 2009 : Accepted September 8, 2009)

Abstract The photocatalysts of Fe-ACF/TiO_2 compositeswere prepared by the sol-gel method and characterized by BET, XRD, SEM, and EDX. It showed that the BET surface area was related to adsorption capacity for each composite. The SEM results showed that ferric compound and titanium dioxide were distributed on the surfaces of ACF. The XRD results showed that Fe-ACF/TiO_2 composite only contained an anatase structure with a Fe mediated compound. EDX results showed the presence of C, O, and Ti with Fe peaks in Fe-ACF/TiO_2 composites. From the photocataytic degradation effect, TiO_2 on activated carbon fiber surface modified with Fe (Fe-ACF/TiO_2) could work in the photo-Fenton process. It was revealed that the photo-Fenton reaction gives considerable photocatalytic ability for the decomposition of methylene blue (MB) compared to non-treated ACF/TiO_2, and the photo-Fenton reaction was improved by the addition of H_2O_2. It was proved that the decomposition of MB under UV (365 nm) irradiation in the presence of H_2O_2 predominantly accelerated the oxidation of Fe^{2+} to Fe^{3+} and produced a high concentration of $OH^{\cdot}$ radicals.

Key words activated carbon fiber, TiO_2, Fe, H_2O_2, photo-Fenton.

1. Introduction

Immobilizing TiO_2 onto activated carbon fibers surface were recently developed and studied.[1-5] It was proved that those photocatalysts could adsorb a large amount of methylene blue (MB) from the aqueous solution due to the porous structure[6-7] and had higher photoactivity for decomposition of MB than the pristine TiO_2 under UV irradiation.[2-3] And some advantages of activated carbon fiber were also found, which attracted more water molecules and/or organic binder on TiO_2 surface and suppression of phase transformation from anatase to rutile during heat treatment at high temperature.

It was also reported that TiO_2 modified with Fe^{3+} could work as photocatalyst for decomposition of organic dye via the photo-Fenton process.[8] The photo-Fenton process has been studied by many researchers, because it can accelerate the degradation of many organic compounds in water via $OH^{\cdot}$ radicals, which are formed during photo-Fenton reactions.[9-12] It was well known that the $OH^{\cdot}$ radicals is a powerful and indiscriminate oxidizing agent for decomposing a wide range of organic compounds.[13-15] Therefore, iron is the most commonly metal used as a Fenton reagent in this process.[16] However, the photo-Fenton process is governed by the amount and ratio of Fe^{2+}/Fe^{3+}, because the oxidation of Fe^{2+} to Fe^{3+} is slow and difficult in acidic solution. In general, the solution of organic dye decomposed with photocatalysts is acidic.[17-18]

H_2O_2 could decompose organic dye to highly hydrophilic products in a very short time, complete mineralization proceeded rather slowly.[19] However, it was reported that H_2O_2 can accelerate the oxidation of Fe^{2+} to Fe^{3+}.[20] When iron exists only in the formation of Fe^{3+} in the catalyst, the Fenton reaction is limited by the reduction of Fe^{3+} to Fe^{2+} due to the presence of H_2O_2, which is considerably slower than the oxidation of Fe^{2+}. Thus, in the presence of Fe^{3+} and H_2O_2, a significant acceleration of the decomposition is obtained after reduction of Fe^{3+}. The other author reported that the initial presence of Fe^{2+} and H_2O_2 could also accelerate the decomposition of organic dye. Although a complex process of oxidation of Fe^{2+} to Fe^{3+} was appeared, but could not affect oxidation of organic dye through radical process significantly. Because at low dose of Fe^{2+} the consumption of H_2O_2 in the initial reaction period is also low, so that the residual H_2O_2 would play

†Corresponding author
E-Mail : wc_oh@hanseo.ac.kr (W. -C. Oh)

an active role in the final oxidation process.[21] As above pointed out, when the decomposition of organic dye depend on photo-Fenton reaction, addition of H_2O_2 to the solution could reduce Fe^{3+} to Fe^{2+}, the rate of decomposition of organic compounds in photo-Fenton process was accelerated by this behavior.

In the present study, photocatalysts of Fe-ACF/TiO_2 composites were prepared by a sol-gel method and were characterized by BET, SEM, XRD and EDX. The photoactivity of Fe-ACF/TiO_2 photocatalysts under UV with or without addition of H_2O_2 towards decomposition of MB was discussed in relation to dyes adsorption on the photocatalyst surface, photocatalytic oxygenation of TiO_2 and reactivity of iron phases in photo-Fenton process.

2. Experimental Procedure

2.1 Materials

Activated Carbon Fiber (ACF) was purchased from EAST ASIS Carbon Fibers Co., Ltd, (Anshan, China), their properties are shown in Table 1. Hydrogen Peroxide (H_2O_2) was purchased from Daejung Chemicals & Metals Co., Ltd, (Korea). Titanium (IV) oxysulfate hydrate ($TiOSO_4 \cdot xH_2O$ (TOS), Sigma-Aldrich, Germany) was selected as a titanium source for the preparation of ACF/TiO_2 composites, and $Fe(NO_3)_3 \cdot 9H_2O$ as the ferric source was purchased from Duksan Pure Chemical Co., Ltd, (Korea). The MB was used as analytical grade which was purchased from Duksan Pure Chemical Co., Ltd, (Korea).

Table 1. The properties of ACFs.

Physical properties	Units
Density	1.23 ~ 1.91 g/mL
Electrical Resistivity	$5.2 \times 10^{-3} \sim 6.8 \times 10^{-3}\ \Omega \cdot cm$
Diameter	12 ~ 15 μ
Tensile Strength	$4 \sim 6 \times 10^8$ Pa
Tensile Modulus	$3 \times 10^{10} \sim 4 \times 10^{10}$ Pa
Elemental carbon	≥ 95 wt%

Table 2. Nomenclatures of non-treated ACF/TiO_2 and Fe-treated ACF/TiO_2 composites.

Samples	Nomenclatures
ACF + Titanium iso propoxide	AT
ACF + $Fe(NO_3)_3$ (0.1M) + TOS	$F_{0.1}AT$
ACF + $Fe(NO_3)_3$ (0.25M) + TOS	$F_{0.25}AT$
ACF + $Fe(NO_3)_3$ (0.5M) + TOS	$F_{0.5}AT$

2.2 Preparation of samples

In this experimental process, first, 10 g ACF was added into to 50 ml 0.1, 0.15 and 0.5 M $Fe(NO_3)_3 \cdot 9H_2O$ solution and the mixtures were stirred 24 h using a non-magnetic stirrer at room temperature. After heat treatment at 773 K, we obtained the Fe-ACF. The Fe-ACF was put into the mixture of TOS and ethanol. Then the mixed solution was stirred for 5 h in an air atmosphere. After stirring solution was transformed to gel state, and these gels were heat treated at 923 K for 1 h. And then the Fe-treated ACF/TiO_2 composites were obtained. The nomenclatures of prepared samples are listed in Table 2. At the same time, an original sample of ACF/TiO_2 was quoted from former experiment[22] and compared with that of Fe-ACF/TiO_2 composites obtained in present study.

2.3 Characteristics and investigations of the samples

The BET surface area by N_2 adsorption method was measured at 77 K using a BET analyzer (Monosorb, USA). XRD (Shimadz XD-D1, Japan) result used to identify the crystallinity by Cu Kα radiation. SEM used to observe the surface state and structure of Fe-ACF/TiO_2 composites using an electron microscope (JSM-5200 JOEL, Japan). EDX spectra were also obtained for determining the elemental information of ACF/TiO_2 and Fe-ACF/TiO_2 composites. UV-vis absorption parameters for the MB solution decomposed by ACF/TiO_2 and Fe-ACF/TiO_2 composites under UV lamp irradiation with H_2O_2 and without H_2O_2 were recorded using a Spectronic (USA) spectrometer.

2.4 Photocatalytic activity of Fe-ACF/TiO_2

The photocatalytic decomposition was tested by different Fe-ACF/TiO_2 composites powder and an aqueous solution of MB in a 100 mL glass container and then irradiating the system with 20W UV light at 365 nm with H_2O_2 and without H_2O_2, which was used at the distance of 100 mm from the solution in darkness, respectively. The sample powder of 0.03 g was suspended in the 50 ml of MB solution with a concentration of 1.0×10^{-5} M. Then, the mixed solution was emplaced in the dark for at least 2 h, in order to establish an adsorption-desorption equilibrium, which was hereafter considered as the initial concentration (c_0) after dark adsorption. Then, experiments were carried out under UV only and under UV with addition of 1.5×10^{-3} mol H_2O_2 to the MB solution (UV and UV + H_2O_2, respectively). Solution was then withdrawn regularly

from the reactor by an order of 30, 60, 90, and 120 min, afterwards, 10 mL of solution was taken out and immediately centrifuged to separate any suspended solids. The clean transparent solution was immediately analyzed by using a UV-vis spectrophotometer in order to decrease continual oxidation of H_2O_2 for MB residue. The intensity at 660 nm for each sample was recorded.

3. Results and Discussion

3.1 Structure and morphology of Fe-treated ACF/TiO_2

The BET data of pristine ACF, ACF/TiO_2 and Fe-ACF/TiO_2 samples are summarized in Table 3. The specific surface area of the as-received ACF was 1842 m^2/g, and almost all BET surface area parameters for the composites have decreased considerably compared with that of pristine ACF. Eventually, it can be evidently seen that there was large change of the micropore size distribution for ACF/TiO_2 and Fe-ACF/TiO_2 composites compared with that of corresponding ACF. This result indicated that the total surface area decreased after formation of TiO_2 particles by Ti precursor treatment. It was considered that the invaded TiO_2 particles can be blocked to pore in ACF. Generally, the BET surface area is thought decrease due to the blocking of the micropores by surface complexes introduced through the formation of the ACF/TiO_2 composites.[23] Especially, for Fe-ACF/TiO_2 composites, the BET surface area was continuously decreased from $F_{0.1}$AT to $F_{0.5}$AT. It indicated that

Fe compounds could also be blocked to pore in ACF as TiO_2 particles, hence to decrease specific surface area. The similar phenomena had also been observed in the references.[24-25]

Fig. 1 shows SEM images of the Fe-ACF/TiO_2 and non-treated ACF/TiO_2. From the results, it is observed that TiO_2 particles were immobilized on the surface of ACF, the fixed TiO_2 particles did not form compact configuration on the ACF surface as shown in Fig. 1. However, the presence of the iron complexes particles could not change this situation due to ionic size. Rather small clusters of TiO_2 crystals spread over the ACF surface with irregular shape, and the interstices among crystalline particles provide an ideal path for the transport and adsorption of organic molecules such as MB which molecular dimension is about $1.70 \times 0.76 \times 0.325$ nm. According to the Fig. 1(e), (f), (g) and (h), it is also observed that the TiO_2 particles were agglomerated on the surface of ACF. In the comparison of different concentrations of Fe in all samples, there was no significant difference. Generally, it is considered that good particle dispersions can produce high photocatalytic activity. In previous studies,[26-27] ACF/TiO_2 composites treated with nitric acid enhanced the homogenous and uniform distribution of TiO_2 particles. Moreover, shown in Fig. 1(a), (b), (e), (f), (g) and (h), some adjacent fibers were connected to each other by the TiO_2 particles deposited. Thus, the less inner space between neighboring fibers created a 3-D environment that could not enable the transport of chemical species in question and UV irradiation.

Fig. 2 shows the XRD patterns of the Fe-ACF/TiO_2 and non-treated ACF/TiO_2. The peaks of all samples at 25.4, 38.2, 47.9, 54.8 and 62.6° are related to the diffractions of the (101), (112), (200), (211), and (204) planes of anatase. No significant diffraction peaks of rutile-phase TiO_2 were detected in the XRD patterns. According to the former studies,[28-29] pure anatase nanocrystallites are very efficient photocatalysts due to their superior photocatalytic properties. Moreover, in the patterns of $F_{0.1}$AT, $F_{0.25}$AT and $F_{0.5}$AT, we can clearly find the peaks of Fe,

Table 3. Specific BET surface areas of pristine ACF and Fe-treated ACF/TiO_2 composite samples.

Samples	S_{BET} (m^2/g)
Pristine ACF	1842
AT	1268
$F_{0.1}$AT	782
$F_{0.25}$AT	745
$F_{0.5}$AT	706

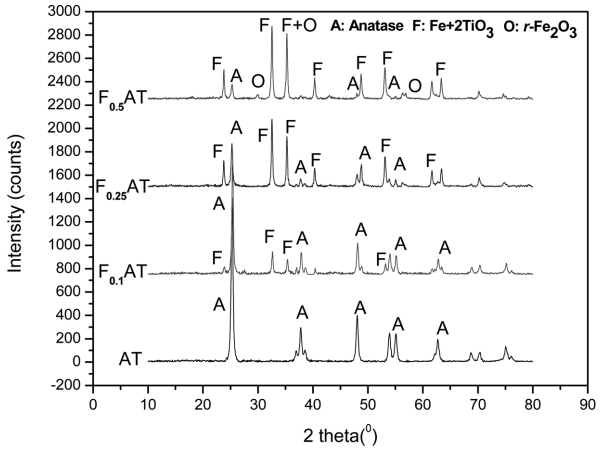

Fig. 2. XRD patterns of powdered ACF/TiO_2 and Fe-ACF/TiO_2 composites.

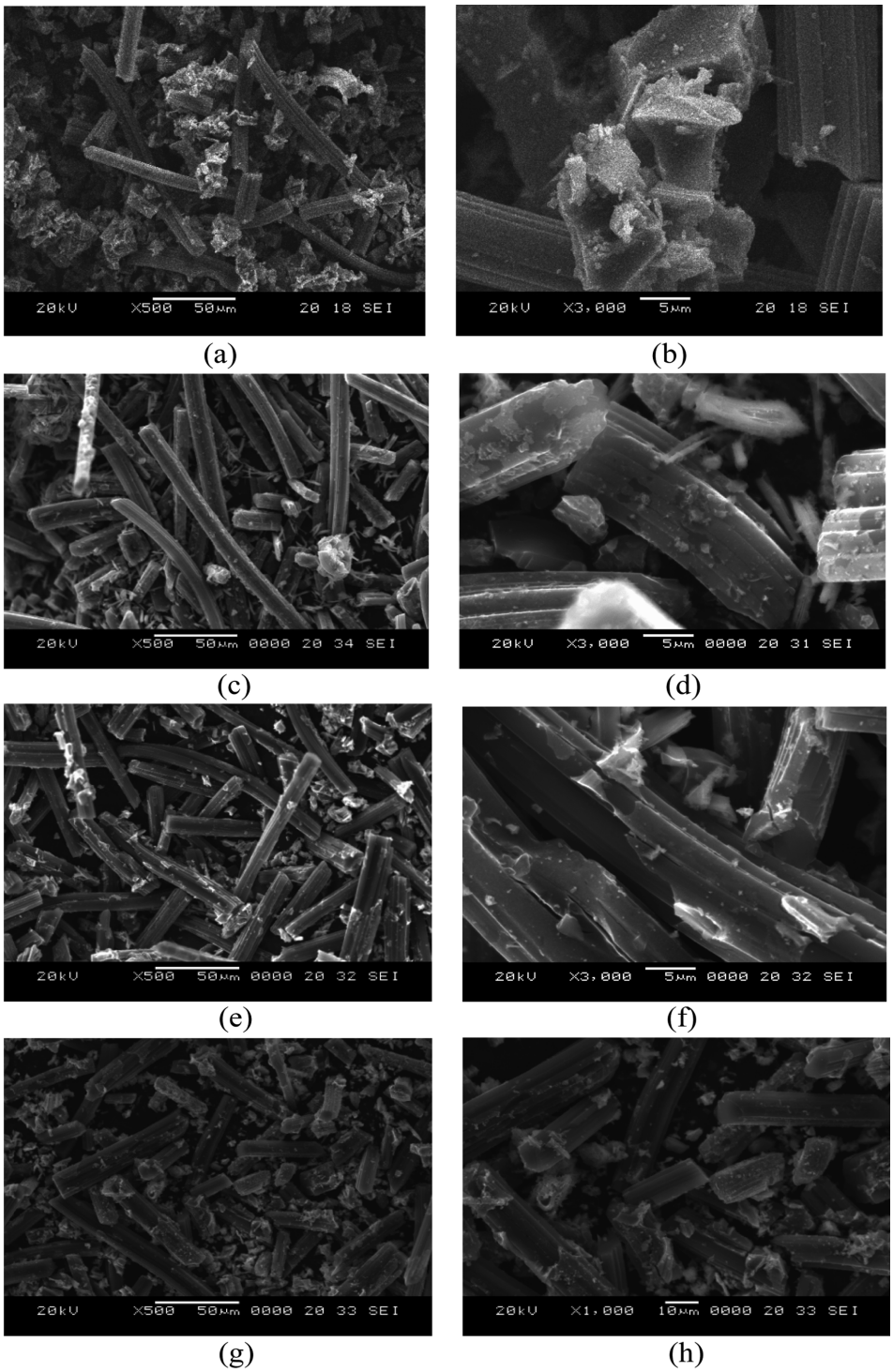

Fig. 1. SEM images of ACF/TiO_2 and Fe-ACF/TiO_2 composites: AT: (a) × 500, (b) × 3000; $F_{0.1}$AT: (c) × 500, (d) × 3000; $F_{0.25}$AT: (e) × 500, (f) × 3000 and $F_{0.5}$AT: (g) × 500, (h) × 3000.

which was further supported by observation of EDX elemental microanalysis of Fe-ACF/TiO_2. Especially, 'γ-Fe_2O_3' diffraction peaks were only found in F3T. The main diffraction peaks have characteristic reflections of (110), (210), and (211).[30] These nanocrystallites were produced by heat treatment temperature at 773-1173 K.[31]

Fig. 3 shows the results of elemental analysis by EDX spectra of Fe-ACF/TiO_2 and non-treated ACF/TiO_2 composites. The spectra show the main presence of C, O and Ti peaks. As expected, the peaks of Fe element were

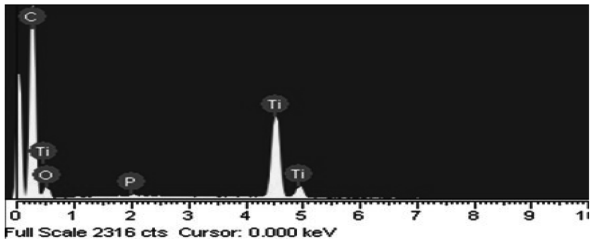

(a)

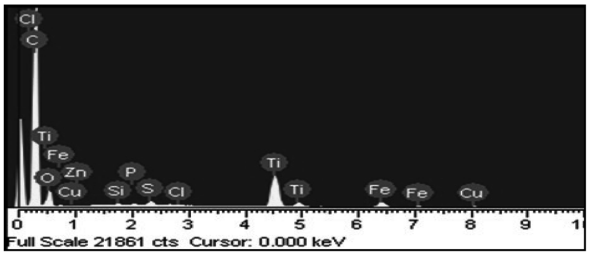

(b)

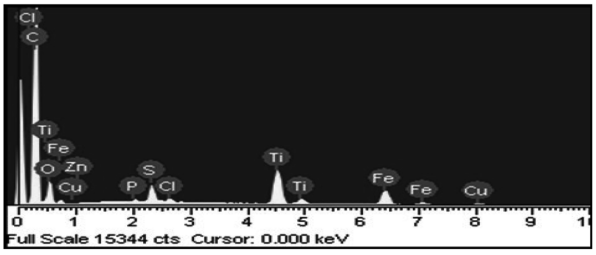

(c)

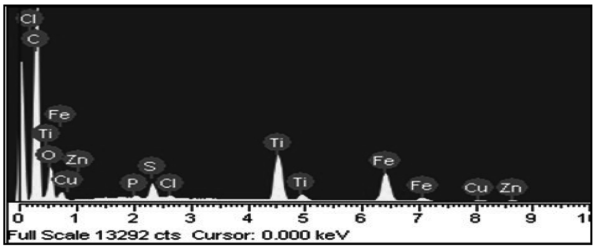

(d)

Fig. 3. EDX elemental microanalysis of non-treated ACF/TiO_2 and Fe-treated ACF/TiO_2 composites: (a) AT, (b) $F_{0.1}$AT (c) $F_{0.25}$AT and (d) $F_{0.5}$AT.

Table 4. EDX elemental microanalysis (wt.%) of non-treated ACF/TiO_2 and Fe-treated ACF/TiO_2 composites.

Samples	Elements			
	C	O	Ti	Fe
AT	53.84	21.79	18.90	0
$F_{0.1}$AT	71.18	16.82	7.8	2.18
$F_{0.25}$AT	67.41.	17.63	6.52	5.18
$F_{0.5}$AT	60.04	21.07	7.53	8.65

observed after the addition of Fe $(NO_3)_3$. The EDX elemental microanalysis (wt. %) of all samples is listed in Table 4. For the Fe-ACF/TiO_2 composites, we observed

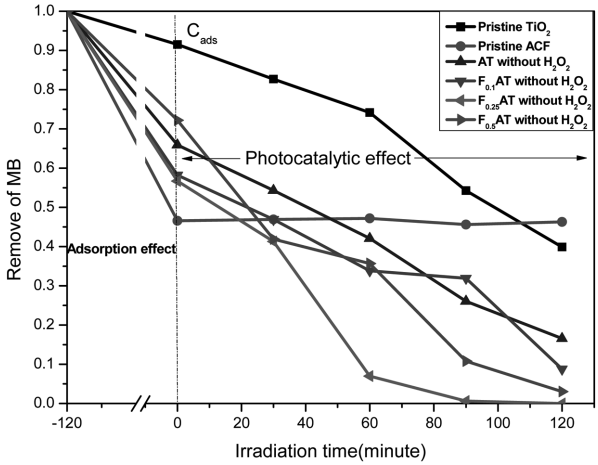

Fig. 4. Removal of MB in the aqueous solution on UV irradiation time without H_2O_2 for the pristine TiO_2, pristine ACF, non-treated ACF/TiO_2 and Fe-ACF/TiO_2 composites.

that stronger peaks of carbon and Ti metal are seen than that of any other elements in most of these spectra.

3.2 Photocatalytic activity

Removal of MB in the aqueous solution on UV irradiation time without H_2O_2 for the non-treated ACF/TiO_2 and Fe-ACF/TiO_2 composites via adsorption and photodecomposition are shown in Fig. 4. ACF was used to probe the adsorption of MB from aqueous solution under dark condition. From Fig. 4, we can know that the pristine ACF showed the strong adsorption capacities due to larger specific surface area. The factors leading to the affected adsorption capacity should involve the change of the surface properties of the ACF and particle dispersions of TiO_2 and/or Fe. As shown in Fig. 4, it is well known that the adsorption capacity of ACF/TiO_2 and Fe-ACF/TiO_2 was decreasing. To evaluate the actual photocatalytic activities strongly depend on TiO_2 and Fe compounds. According to the Fig. 4, the degradation effect of ACF/TiO_2 is higher than the original TiO_2, it is considered that the ACF can fleetly transfer electron to reduce electronic accumulation on TiO_2 particles, it is quite reasonable to describe the combination effect, which is in agreement with previous study.[4] And integrating the EDX data of ACF/TiO_2 and Fe-ACF/TiO_2 series, the efficiency of MB decomposition was increased distinctly though content of Ti was highest in non-treated ACF/TiO_2 sample. It is noteworthy that the Fe modified ACF-TiO_2 enhances the photocatalytic activity greatly. This reaction could be attributed to photo-Fenton reaction, which is showed in Eq (1):

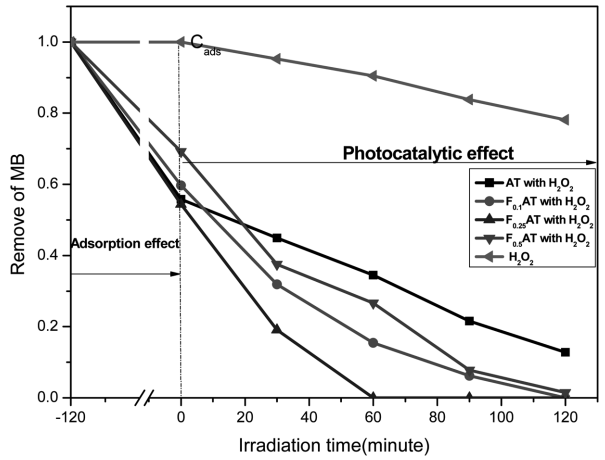

Fig. 5. Removal of MB in the aqueous solution on UV irradiation time without H_2O_2 for the non-treated ACF/TiO_2 and Fe-ACF/TiO_2 composites.

$$Fe^{3+} + OH^- + hv \rightarrow Fe^{2+} + OH^{\cdot} \quad (1)$$

However, the photocatalytic activity of $F_{0.5}$AT was lower than that of $F_{0.25}$AT. It is attribute to the superfluous irons can act as recombination centers for the electron/hole pairs.[32)]

Removal of MB in the aqueous solution on UV irradiation time with H_2O_2 for non-treated ACF/TiO_2 and Fe-ACF/TiO_2 composites are presented in Fig. 5. When H_2O_2 (1.5×10^{-3} mol) is only added to the MB solution under UV light. In the previous papers,[16,19,33)] decomposition of phenol solution using H_2O_2 under UV irradiation without photocatalysts was progressed fast, The higher reaction rates of H_2O_2 can be attributed to the increase in the concentration of hydroxyl radicals. These radicals are generated by Eq. (6):

$$H_2O_2 + hv \rightarrow 2\ OH^{\cdot} \quad (6)$$

In this experiment results, however, decomposition of MB is slow. It might be attributed that the formation of $OH^{\cdot}$ radicals by H_2O_2 was not sufficient to achieve complete decomposition of MB molecules, its production of decomposition still contained ring-retaining intermediates within 120 min under UV irradiation.

Comparison of Fig. 4 and Fig. 5 results, a quite different behavior of photocatalytic activity was observed on the photocatalysts of non-treated ACF/TiO_2 and Fe-ACF/TiO_2 in the presence of H_2O_2. However, the photocatalytic activity of non-treated ACF/TiO_2 with and without H_2O_2 is little variation. It can be explained that deposition of ACF on the site of $OH^{\cdot}$ could cause decreasing the yield of $OH^{\cdot}$ radicals which are mainly generated by the reaction of photoinduced holes in TiO_2 with the adsorbed molecular water on its surface. These reactions are showed by Eqs (2)-(4).

$$TiO_2 + hv \rightarrow h^+ + e^- \quad (2)$$

$$h^+H_2O_{(ads)} \rightarrow OH^{\cdot}{}_{(ads)} + H^+_{(ads)} \quad (3)$$

$$OH^{\cdot}{}_{(ads)} + H_2O_2 \rightarrow HO_2^{\cdot} + H_2O \quad (4)$$

$OH^{\cdot}$ radicals formed on the surface of TiO_2 was suppressed by the scavenging of the free carriers by H_2O_2. Additionally a part of H_2O_2 was adsorbed on the ACF surface, and the formation of $OH^{\cdot}$ radicals by photolysis of H_2O_2 was lower.

On Fe-ACF/TiO_2 composites, decomposition of MB was significantly increased. It can be considered that the addition of H_2O_2 into the reaction solutions caused oxidation of Fe^{2+} and more formation of $OH^{\cdot}$ radicals. The reaction is showed in Eq (5):

$$Fe^2 + H_2O_2 \rightarrow Fe^{3+} + OH^- + OH^{\cdot} \quad (5)$$

As shown in Eq (5), Fe^{3+} can be reduced to Fe^{2+} with an increase of $OH^{\cdot}$ radical due to addition of H_2O_2. On the other hand, the photo-Fenton process can be efficiently recycled.

The presence in Fe-ACF/TiO_2 caused the decomposition of MB is more progressed fast by powerful H_2O_2 assisting photo-Fenton reaction.

In contrast, in case of $F_{0.1}$AT, $F_{0.25}$AT and $F_{0.5}$AT for decomposition of MB via addition of H_2O_2, they indicated various degrees increase of the photocatalytic activity. However, we observed that the active decomposition of $F_{0.5}$AT was slower than that of $F_{0.1}$AT and $F_{0.25}$AT. It could be attributed to the different reaction of MB decomposition occurred on $F_{0.5}$AT composite due to $F_{0.5}$AT contained superfluous Fe. The reaction is generated by Eqs. (7)-(8).

$$Fe^{3+} + H_2O_2 \rightarrow Fe(HO)_2^+ \quad (7)$$

$$Fe(HO)_2^+ \rightarrow Fe^{2+} + HO_2^{\cdot} + H^+ \quad (8)$$

The yielding $HO_2^{\cdot}$ radicals cannot effectively decompose MB molecules as above mentioned.

4. Conclusion

The Fe-ACF/TiO_2 composites were prepared by a sol-gel method. From the SEM, the particles of TiO_2 aggregated

into clusters were fixed on the surface of ACF. XRD patterns of the composites showed that TiO_2 exists as a typical single and clear anatase phase. The EDX spectra showed the main peaks of C, O, and Ti, for the Fe-ACF/TiO_2 composites. And, we observed the peaks of the Fe element. Modification of TiO_2 photocatalyst by ACF and Fe could enhance photoactivity for decomposition of MB under the condition of UV via photo-Fenton process. The Fe-ACF/TiO_2 composites seems to be beneficial for decomposition of MB under UV with H_2O_2, It is suggested that the deomposition of MB in Fe-ACF/TiO_2 photocatalyst systems is accelerated by forming more $OH^{\cdot}$ radicals.

References

1. J. W. Shi, Chem. Engi J., **151**, 241 (2009).
2. Y. N. Hou, J. H. Qu, X. Zhao, P. J. Lei, D. J. Wan, and C. P. Huang, Sci. Total Environ., **407**, 2431 (2009).
3. D. Q. Mo, and D. Q. Ye, Sur & Coatings Technol., **203**, 1154 (2009).
4. W. C. Oh, F. J. Zhang, M. L. Chen, Y. M. Lee, and W. B. Ko, J. Indust. Engin. Chem., **15**, 190 (2009).
5. L. F. Liu, G. H. Zheng and F. L. Yang, Chem. Engi. J., doi:10.1016/j.cej.2009.04.008.
6. W. C. Oh and M. L. Chen, J. Ceram. Process. Res., **9**(2), 100 (2008).
7. M. L. Chen, C. S Lim, and W. C. Oh, Carbon let., **8**(3), 177 (2007).
8. M. Pera-Titus, V. Garc′l a-Molina, M. A. Baños, J. Giménez, and S. Esplugas, Appl. Catal. B: Environ., **47**, 219 (2004).
9. M. Neamtu, A. Yediler, I. Siminiceanu, and A. Kettrup, J. Photochem. and Photobiol A: Chem., **161**, 87 (2003).
10. M. I. Franch, J. A. Ayllón, J. Peral, and X. Domènech, Appl. Catal. B: Environ., **50**, 89 (2004).
11. H. Fallmann, T. Krutzler, R. Bauer, S. Malato, and J. Blanco, Catal. Today., **54**, 309 (1999).
12. R. Bauer, G. Waldner, H. Fallmann, S. Hager , M. Klare, T. Krutzler, S. Malato, and P. Maletzky, Catal, Today, **53**, 131 (1999).
13. J. H. Carey, J. Lawrence, and H. M. Tosine, Bull. Environ. Contam. Toxicol., **16**, 697 (1976).
14. V. A. Nadtochenko, A. G. Rincon, S.E. Stanca, and J. Kiwi, J. Photochem. Photobiol. A: Chem., **169**, 131 (2005).
15. A. Fujishima, T. N. Rao, and D. A. Tryk, J. Photochem. Photobiol. C., **1**, 1 (2000).
16. B. Tryba, A. W. Morawski, M. Inagaki, and M. Toyoda, Chemosphere, **64**, 1225 (2006).
17. C. Guillard, H. Lachheb, A. Houas, M. Ksibi, E. Elaloui, and J. M. Herrmann, J. Photochem and Photobiology A: Chem., **158**, 27 (2003).
18. M. Carrier, N. Perol, J. M. Herrmann, C. Bordes, S. Horikoshi, J. O. Paisse, R. Baudot and C. Guillard, Appl. Cata.B: Environ., **65**, 11 (2006).
19. B. Tryba, A. W. Morawski, M. Inagaki, and M. Toyoda, Appl. Catal. B: Environ., **63**, 215 (2006).
20. M. Pera-Titus, V. Garcia-Molina, M. A. Ban˜os, J. Gime´nez, and S. Espluga, Appl. Catal. B: Environ., **47**, 219 (2004).
21. F. He, L. Lei,. J., Zhejiang, Univ. Sci., **5**, 198. (2004)
22. Y. G. Go, F. J. Zhang, M. L. Chen, and W. C. Oh, J. Mater. Res., **19**(3), 142 (2009).
23. J. W. Shi, J. T. Zheng, P. Wu and X. J. Ji, Catal. Communications., **9**. 1846-C1850. (2008).
24. F. J. Zhang, M. L. Chen and W. C. Oh, Kor. J. Mater. Res., DOI: 10.3740/MRSK.2008.18.9.000.
25. W. D Wang, P. Serp, P. Kalck and J. L. Faria, J. Mole. Catal. A: Chem., **235**, 194 (2005).
26. W. C. Oh, and M. L. Chen, J. Ceram. Proc. Res., **8**, 316 (2007).
27. W. C. Oh, S. B. Han, and J. S. Bae, Analytical Science & Technol., **20**(4), 279 (2007).
28. D. C. Hurum, K. A. Gray, T. Rajh, and M. C. Thurnauer, J. Phys. Chem. B., **109**, 977 (2005).
29. C. G. Silva and J. L. Faria, J. Molecular Cata. A: Chem., **305**, 147 (2009).
30. S. Chaianansutcharit, O. Mekasuwandumrong, and P. Praserthdam, Cer. International., **33**, 697 (2007).
31. K. Hayashi, W. Sakamoto, and T. Yogo, J. Magnetism and Magnetic Mater., **321**, 450 (2009).
32. W. C. Hung, Y. C. Chen, H. Chu, and T. K. Tseng, Appl.Sur. Sci., **255**, 2205 (2008).
33. B. Tryba, J. Hazar. Mat., **151**, 623 (2008).